Optical Diffraction in Chiral Smectic-C Liquid Crystals

K. A. Suresh, Yuvaraj Sah, P. B. Sunil Kumar, and G. S. Ranganath
Raman Research Institute, Bangalore 560080, India
(Received 17 September 1993)

We report a study on the optical diffraction for light propagation perpendicular to the twist axis in the chiral smectic-C liquid crystal. In this phase grating mode, we find very unusual intensity and polarization features in the diffraction pattern. These observed features can be explained by invoking the theory of anisotropic gratings which takes into account the internal diffractions.

PACS numbers: 42.70.Df, 42.25.Fx

The chiral smectic-C (S_{C^*}) liquid crystal phase has a helical stack of layers of uniformly tilted molecules. The tilt of the molecules is coupled to the layer thickness producing local biaxiality in the medium. The chirality in the medium removes the mirror symmetry in the system leading to the possibility of sustaining an electric polarization **P** (along the local twofold axis), spiraling uniformly about the twist axis of the helical structure. Meyer *et al.* [1] discovered the existence of ferroelectricity in S_{C^*}. Technologically, S_{C^*} became very important after Clark and Lagerwall [2] demonstrated the submicrosecond dynamics and other related properties like symmetric bistability, threshold behavior, and large electro-optic response that are exploited in the fast switching display devices. Further, studies on pyroelectricity [3], shear induced polarization [4], electroclinic effect [5], second harmonic generation [6], and other phenomena [7] have established the rich physical properties exhibited by S_{C^*}. In addition, S_{C^*} has many interesting optical properties. These arise due to the fact that in the successive layers, the local index ellipsoid (triaxial ellipsoid) spirals uniformly about the twist axis at a constant angle. The study of propagation of light in the Bragg reflection mode has shown some distinct optical polarization properties peculiar to this phase [8–11]. The study of propagation of light perpendicular to the twist axis is equally interesting, but has drawn very little attention. In this geometry, the medium acts as a phase grating; i.e., a plane wave front incident on the sample becomes a periodically corrugated wave front inside the medium resulting in optical diffraction. So far, optical studies in this geometry have been largely confined to the determination of the pitch of the structure [12]. We have undertaken a study of the propagation of light in S_{C^*} in the phase grating mode in all its details.

In this Letter, we report for the first time some unusual features of diffraction associated with the phase grating mode in S_{C^*}. We observed that in a range of sample thicknesses, the diffracted light in all the orders was preferentially polarized parallel to the twist axis. Further, in thicker samples, although the above features were seen at lower temperatures, at higher temperatures the diffracted light in all the orders was nearly polarized perpendicular to the twist axis. These observed features contradict the predictions of the Raman-Nath theory of phase gratings [13] as extended to S_{C^*} [14] where the wave front corrugations inside the medium are ignored. It is shown here that a rigorous theory of anisotropic dielectric gratings as developed by Rokushima and Yamakita (RY) [15] can account for our observed features.

The experiments were carried out on the commercially obtained sample BDH SCE-6. This has the following sequence of transitions:

$$\text{Crystal} \underset{-15^\circ\text{C}}{\rightarrow} S_{C^*} \underset{63^\circ\text{C}}{\leftrightarrow} \text{Smectic-}A \underset{84^\circ\text{C}}{\leftrightarrow} \text{Cholesteric} \underset{120^\circ\text{C}}{\leftrightarrow} \text{Isotropic}.$$

To get monodomain samples suitable for phase grating geometry, the following procedure was employed: Sample cells were prepared using glass plates which were previously treated with polyimide and rubbed in the parallel direction. Cells of thicknesses 23, 50, 125, and 250 μm were obtained using Mylar spacers. Later, the cells were filled with the sample in the isotropic phase and then cooled very slowly through the cholesteric to smectic-A (S_A) phase in the presence of a magnetic field of strength 2.4 T applied parallel to the rubbed direction of the glass plates. In the S_A phase, the field was removed. Observations under a Leitz polarizing microscope revealed the formation of a very good homogeneous monodomain S_A phase which on further slow cooling transformed to the S_{C^*} phase. In S_{C^*} we got a pattern having uniform parallel striations (fringes). The striations were perpendicular to the rubbed direction of the glass plates and were parallel to the smectic layers. They arise due to a uniformly twisted stack of layers (of tilted molecules) with the twist axis along the rubbed direction. The fringe width corresponds to the pitch of the helical structure [12]. In SCE-6, the pitch varies from about 4 to 6 μm in the temperature range of 25 °C to 60 °C. For samples of thicknesses much lower than 23 μm, due to the surface effects, the helical structure got considerably distorted and hence was not used. In the experimental setup, the cell was kept on the central table of a goniometer which had a 2 mW He-Ne laser ($\lambda = 0.6328$ μm) on the fixed arm. The light was allowed to fall normally on the sam-

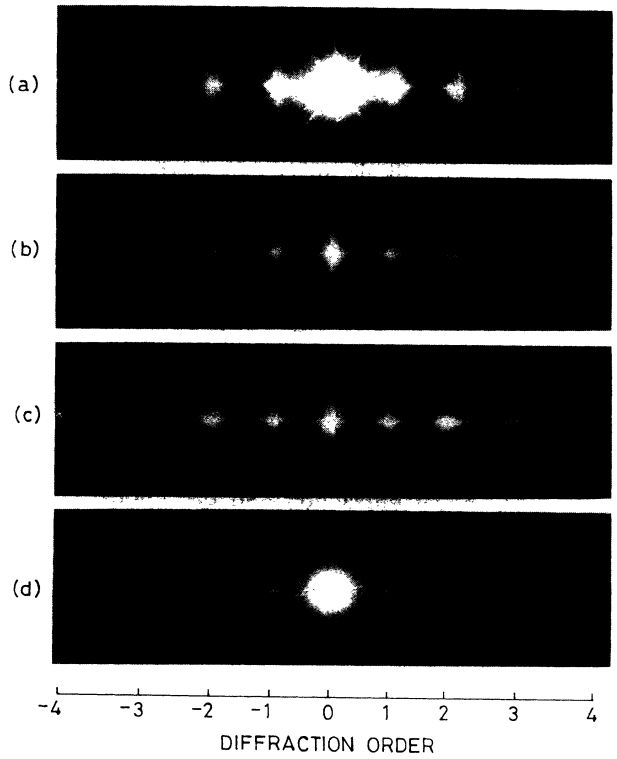

FIG. 1. The photographs of the diffraction pattern of a 50 μm sample at room temperature ($\approx 25\,^{\circ}$C) in (a) HH, (b) HV, (c) VH, and (d) VV geometries. One may note that in (c) the second order is more intense than the first order. Such effects are characteristic of phase gratings. In S_{C^*}, they are sensitive to temperature.

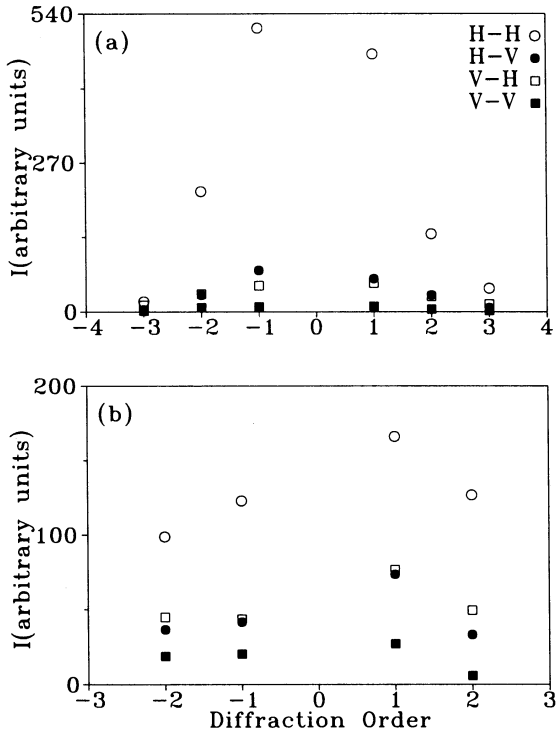

FIG. 2. The intensity I (arbitrary units) in the diffraction orders shown for various geometries for two samples: (a) thickness = 50 μm and temperature = 50.6 °C; (b) thickness = 250 μm and temperature = 45.5 °C. Here one may notice that in every order $I(HH) > I(HV)$ and $I(VH) > I(VV)$. The intensity of the direct beam is too high to be shown here. The asymmetry in the intensity pattern for some orders is due to slight imperfections in the orientation of the sample.

ple cell. The diffracted light was collected on a photodiode mounted on the moving arm and measured with a Keithley 181 nanovoltmeter. Simultaneously the signal was fed into a Graphtec servocorder.

In our experiments, for incident linearly polarized light, we got sharp diffraction spots. Typically there were 6 to 7 orders on either side of the direct beam. Figure 1 shows one such diffraction pattern in the geometries HH, HV, VH, and VV. (H denotes linear polarization parallel to the twist axis and V denotes linear polarization perpendicular to the twist axis. The first symbol indicates the state of polarization of the incident light and the second symbol indicates the polarization state in which the diffracted beam was analyzed.)

Figure 2 shows the measured diffracted intensity in the various orders (except the zeroth order) for 50 and 250 μm sample thicknesses. Surprisingly, the intensity in the HH geometry (open circles) is very much higher than the intensity in the HV geometry (closed circles) for all orders. Also the intensity in the VH geometry (open squares) is higher than that in the VV geometry (closed squares). That is, in all these orders, the diffracted light is nearly linearly polarized parallel to the twist axis. Interestingly, this behavior is observed in samples of thickness 23 and 50 μm at all temperatures. For 125 μm the same behavior is also seen at all temperatures except in the neighborhood of the S_{C^*}-S_A transition. However, in the sample with a thickness of 250 μm, a more interesting behavior is found. At temperatures $\lesssim 46\,^{\circ}$C the intensity and polarization features are the same as that described above. But at higher temperatures, the behavior gets completely reversed. This is shown in Fig. 3. Here the intensity of the diffracted light in the VV geometry becomes more intense than the intensity in the VH geometry. Also the intensity in the HV geometry is more than that in the HH geometry; i.e., in this case, in all these orders, the component of the diffracted light perpendicular to the twist axis is more than the component parallel to the twist axis. However, in all these geometries, in all the samples, the zeroth order is in a polarization state close to that of the incident vibration. We have shown data on two samples [Figs. 2(a) and 3] of different thicknesses (50 and 250 μm) but at the same temperature (50.6 °C) to highlight their contrasting behavior.

The above results cannot be accounted for by the

theory [14] of the optical diffraction in S_{C^*} which assumes that in the corrugated wavefront, inside the medium, the amplitude of the corrugation is much smaller than the wavelength of the corrugation; i.e., the internal diffractions are ignored. This assumption is valid only in the limit of low birefringence and small thickness. However, in the present case, the material has a high birefringence and the sample thicknesses are large. Hence we have used a more rigorous theory of anisotropic dielectric gratings due to RY [15] which incorporates the internal diffractions within the medium.

Following RY [15] and Galatola, Oldano, and Sunil Kumar [16], the Maxwell equations are written in the form

$$\Psi(z)=\exp(ik_{0z}D)\Psi(0)\,, \tag{1}$$

where

$$\Psi=(E_xH_yE_yH_z)^t$$

and

$$k_0=2\pi/\lambda\,.$$

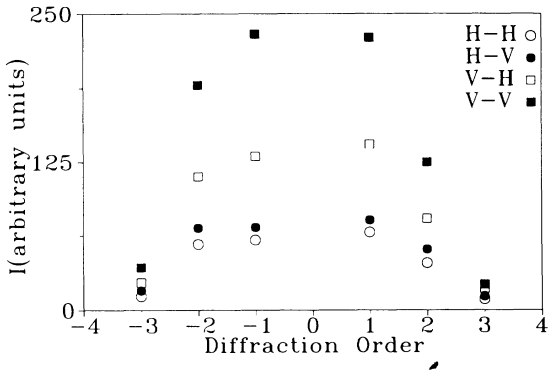

FIG. 3. The intensity I (arbitrary units) in the diffraction orders shown for various geometries for a 250 μm sample at 50.6 °C. One may notice that in every order $I(HH)<I(HV)$ and $I(VH)<I(VV)$.

E_x, E_y, H_x, and H_y are infinite column matrices containing the various Fourier components of the transverse fields and λ is the wavelength of light. The propagation matrix D for our problem simplifies to an infinite square matrix:

$$D=\begin{bmatrix} 0 & I & 0 & 0 \\ \varepsilon_{xx}-\varepsilon_{xz}\varepsilon_{zz}^{-1}\varepsilon_{xz}-Q^2 & 0 & \varepsilon_{xy}-\varepsilon_{xz}\varepsilon_{zz}^{-1}\varepsilon_{zy} & -\varepsilon_{xz}\varepsilon_{zz}^{-1}Q \\ -Q\varepsilon_{zz}^{-1}\varepsilon_{zx} & 0 & -Q\varepsilon_{zz}^{-1}\varepsilon_{zy} & I-Q\varepsilon_{zz}^{-1}Q \\ \varepsilon_{yx}-\varepsilon_{yz}\varepsilon_{zz}^{-1}\varepsilon_{zx} & 0 & \varepsilon_{yy}-\varepsilon_{yz}\varepsilon_{zz}^{-1}\varepsilon_{zy} & -\varepsilon_{yz}\varepsilon_{zz}^{-1}Q \end{bmatrix}.$$

Here, ε_{xz}, etc. are themselves infinite square matrices. The ijth element of the matrix ε_{xz}, etc. is the $(i-j)$th Fourier component of the ε_{xz}, etc. element of the dielectric tensor ε. Q is an infinite diagonal matrix with elements q_0+nq, where q_0 is the incident wave vector in the bounding isotropic medium and q is the grating wave vector with n going from $-\infty$ to ∞; I is the infinite unit matrix.

To compare the theory with the experimental results it is convenient to work in terms of the modes in the bounding isotropic media. If Φ is a vector whose components are the strengths of the different modes in the bounding isotropic media, then Eq. (1) becomes

$$\Phi(z)=S\Phi(0)\,, \tag{2}$$

where S is the scattering matrix whose components are functions of the material parameters. The vector $\Phi(0)$ contains the reflected Φ_r and incident Φ_i components, while $\Phi(z)$ contains the transmitted component Φ_t [16]. A suitable rearrangement in the elements of the Φ vector leads to

$$\Phi_r=\mathcal{R}\Phi_i,\quad \Phi_t=\mathcal{T}\Phi_i\,, \tag{3}$$

where $\mathcal{R}$ and $\mathcal{T}$ are the backward and forward scattering matrices, respectively.

It was sufficient to have the Fourier components up to $n=5$ in the dielectric tensor and also to assume local uniaxiality. Computations with higher Fourier components and biaxiality did not alter our main results. Figure 4 shows the computed results. Here the intensity of the first order is depicted as a function of sample thickness in the different geometries. The intensity in the HH geometry, in the thickness range 50 to 200 μm, is more than that in the HV geometry [Fig. 4(a)], whereas the intensity in the VH geometry is throughout more than that in the VV geometry [Fig. 4(b)]. This is in accordance with the observed results shown in Fig. 2. Further, Fig. 4(a) shows that around 250 μm the intensity behavior in the HH and HV geometry can get reversed. This explains the contrasting behavior in the HH and HV geometries of the 250 μm sample at 45.5 °C [Fig. 2(b)] and at 50.6 °C (Fig. 3). However, the observed results in VV and VH geometries of the 250 μm sample at 50.6 °C are not in accordance with the computed results shown in Fig. 4(b). Also, our observed results for 23 μm, at all temperatures, show the HH component to be greater than the HV component and this is not in accordance with the result shown in Fig. 4(a). It may be pointed out that the computations shown in Fig. 4 are for one set of material parameters. These parameters are sensitive functions of

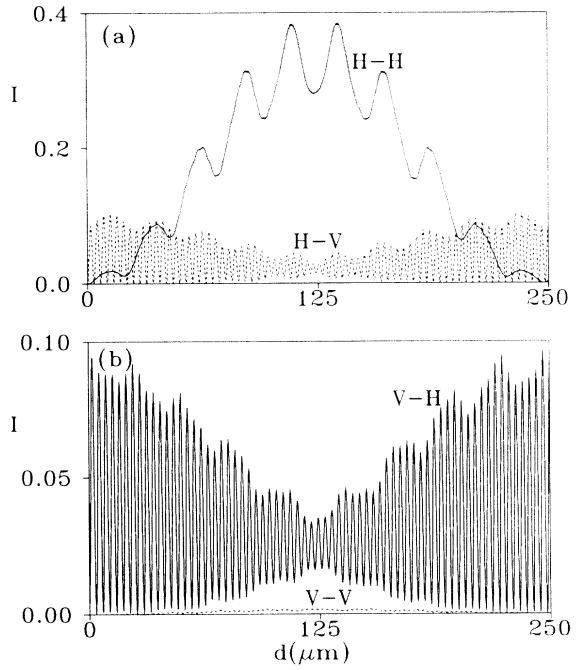

FIG. 4. The normalized intensity I as a function of sample thickness d (μm) for different geometries in the first order. In these computations, the following material parameters of SCE-6 have been used: birefringence = 0.18, pitch = 5 μm, and tilt angle = 18°.

the temperature. It was found that the theory can yield qualitatively all the above observed results by a proper choice of material parameters. Also, the computations show that the RY theory can account for the observed polarization features of the zeroth order as well as those of the higher diffraction orders.

The other interesting feature in Fig. 4 is the appearance of modulations. These modulations in the diffracted intensity can be interpreted as being due to the different orders of scattering. This can be shown by using a perturbation theory [16] where the z-dependent (the propagation direction) part of the dielectric tensor is treated as a perturbation over an effective anisotropic homogeneous medium.

In conclusion, we have experimentally studied, for the first time, the polarization and intensity features of the diffraction in the phase grating mode in S_{C^*}. The observed results are very surprising and interesting and these can be accounted for on the basis of the RY theory.

[1] R. B. Meyer, L. Liebert, L. Strzelecki, and P. Keller, J. Phys. (Paris), Lett. **36**, L69 (1975).
[2] N. A. Clark and S. T. Lagerwall, Appl. Phys. Lett. **36**, 899 (1980).
[3] L. J. Yu, H. Lee, C. S. Bak, and M. M. Labes, Phys. Rev. Lett. **36**, 388 (1976).
[4] P. Pieranski, E. Guyon, and P. Keller, J. Phys. (Paris) **36**, 1005 (1975).
[5] S. Garoff and R. B. Meyer, Phys. Rev. Lett. **38**, 848 (1977).
[6] N. M. Shtykov, M. I. Barnik, L. A. Beresnev, and L. M. Blinov, Mol. Cryst. Liq. Cryst. **124**, 379 (1985).
[7] J. E. Maclennan, N. A. Clark, M. A. Handschy, and M. R. Meadows, Liquid Crystals **7**, 753 (1990).
[8] D. W. Berreman, Mol. Cryst. Liq. Cryst. **22**, 175 (1973).
[9] C. Oldano, Phys. Rev. Lett. **53**, 2413 (1984).
[10] K. Rokushima and J. Yamakita, J. Opt. Soc. Am. A **4**, 27 (1987).
[11] H. L. Ong, Phys. Rev. A **37**, 3520 (1988).
[12] Ph. Martinot-Lagarde, J. Phys. (Paris), Colloq. **37**, C-129 (1976); K. Kondo, F. Kobayashi, H. Takezoe, A. Fukuda, and E. Kuze, Jpn. J. Appl. Phys. **19**, 2293 (1980).
[13] C. V. Raman and N. S. Nagendra Nath, Proc. Indian Acad. Sci. A **2**, 406 (1935).
[14] K. A. Suresh, P. B. Sunil Kumar, and G. S. Ranganath, Liq. Cryst. **11**, 73 (1992).
[15] K. Rokushima and J. Yamakita, J. Opt. Soc. Am. **73**, 901 (1983).
[16] P. Galatola, C. Oldano, and P. B. Sunil Kumar, J. Opt. Soc. Am. A (to be published).

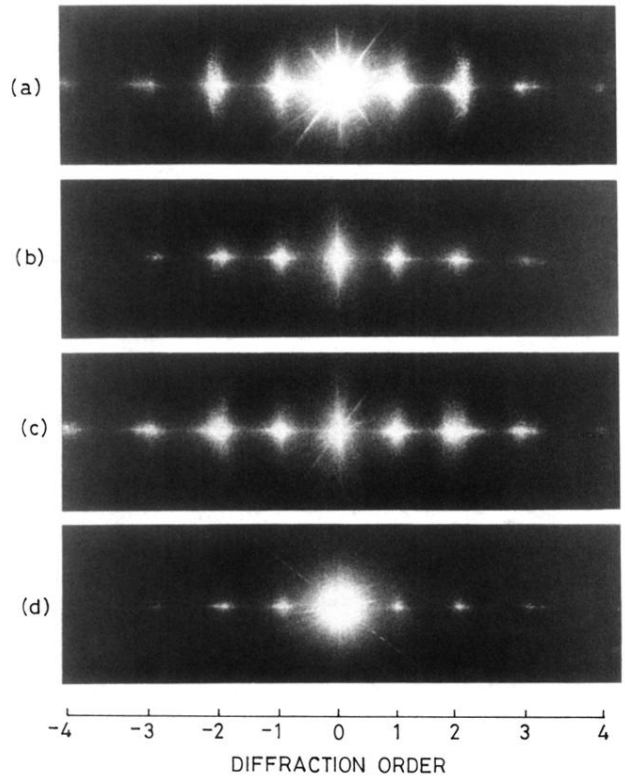

FIG. 1. The photographs of the diffraction pattern of a 50 μm sample at room temperature ($\approx 25\,^{\circ}$C) in (a) *HH*, (b) *HV*, (c) *VH*, and (d) *VV* geometries. One may note that in (c) the second order is more intense than the first order. Such effects are characteristic of phase gratings. In S_{C^*}, they are sensitive to temperature.